Structural and magnetic phase transitions of Fe on stepped Cu(111)

J. Shen, M. Klaua, P. Ohresser, H. Jenniches, J. Barthel, Ch. V. Mohan, and J. Kirschner
Max-Planck-Institut für Mikrostrukturphysik, Weinberg 2, 06120 Halle, Germany
(Received 19 May 1997)

The magnetism and its correlation with morphology and structure of ultrathin Fe/Cu(111) films have been studied. At room temperature, the films grow in a quasi-one-dimensional form (stripes) in the submonolayer range. Between 1.4 and 1.8 ML the stripes percolate and become two-dimensional films. The remanent magnetization of the percolated films was observed to be significantly more stable with respect to time than that of the stripes. At low thickness (<2.3 ML) the films adopt the fcc structure from the substrate and later transform to bcc(110) structure with Kurdjumov-Sachs orientation. Experimental evidence suggests that the fcc films have a low-spin ferromagnetic or ferrimagnetic phase, and a perpendicular easy magnetization axis. The magnetization switches to an in-plane high-spin phase after the fcc to bcc structural transformation has been accomplished. [S0163-1829(97)02541-1]

I. INTRODUCTION

The step decoration effect of Fe growth on Cu(111) has been noticed for some years since the first scanning tunneling microscopy (STM) study on this system.[1] Recently this effect has been used by the authors to produce one-dimensional (1D) Fe stripes on a stepped Cu(111) substrate.[2] It has been found that in the submonolayer regime the deposited Fe atoms form parallel stripes along the step edges. The magnetism of the stripes has a superparamagnetic nature which is distinguished from that of a two-dimensional (2D) ferromagnetic film mainly by its time-dependent remanent magnetization. Further increase in the thickness leads to an increase of the width of the stripes and finally results in the two-dimensional percolation of the films. This system has provided an opportunity to study the transition from 1D to 2D magnetism.

In addition the Fe/Cu(111) films have fcc structure in the low thickness limit,[3,4] which otherwise does not exist below 1100 K in bulk. The magnetism of fcc γ-iron appears to be very interesting. Theoretical calculations have shown that fcc γ-iron may be nonmagnetic, antiferromagnetic, low-spin, or high-spin ferromagnetic depending on the lattice parameters.[5] Though experimental evidence from the bulk indicates that fcc γ-Fe has a antiferromagnetic ground state,[6] the ultrathin films of γ-Fe on Cu(100) were observed to have a high-spin ferromagnetic phase at low thickness (<5 ML).[7] This high-spin ferromagnetic (FM) phase has been associated with the tetragonal distortion of the Fe fcc structure leading to an enlarged atomic volume.[8] To find out whether the high-spin FM phase is a general feature of 2D γ-Fe (ultrathin films), it is important to study the magnetic properties of γ-Fe on a copper substrate with another orientation, such as the (111) plane.

In contrast to the Fe/Cu(100) system, the structure and the magnetism of the Fe/Cu(111) system has been much less understood due to the very limited amount of work. So far it has been reported that at room temperature Fe grows pseudomorphically up to 4 or 5 monolayers,[4] and then transforms to the bcc structure with (110) orientation.[4,9–13] STM has shown that the growth of Fe on Cu(111) is in a three-dimensional manner at room temperature.[1,14] Magnetic measurements from a copper capped Fe/Cu(111) film suggested that the Fe has a surprisingly small magnetic moment ($\sim 0.6\mu$B).[11] The easy magnetization direction, however, appeared to depend strongly on the growth temperature.[11] An electron-capture spectroscopy study has reported the existence of long-ranged ferromagnetic order in a 4-ML film and short-ranged ferromagnetic order in one- or two-monolayer films.[15]

The aim of this work is to systematically study the structural and magnetic properties of the Fe/Cu(111) films with emphasis on the correlation between the structure and their magnetism. *In situ* STM, low-energy electron diffraction (LEED) with intensity vs energy function (I/V LEED) and magneto-optical Kerr effect (MOKE) have been used to study the thickness dependence of the morphology, atomic structure, and magnetism, respectively. The main results are summarized as follows.

(1) In the submonolayer range the Fe films have a quasi-1D form which is characterized by parallel aligned stripes. The remanent magnetization of the stripes was observed to be time dependent.

(2) Between 1.4 and 1.8 ML the Fe stripes percolate to form 2D films. The magnetization relaxation time of the 2D films is significantly longer than that of the 1D films.

(3) We proved the occurrence of the fcc to bcc transition. The critical thickness is between 2.3 and 2.7 ML, which is somewhat lower than the previously reported 4 or 5 ML.[4]

(4) The easy magnetization axis switches from perpendicular to in-plane between 2.3 and 3.0 ML, in coincidence with the fcc to bcc structural transition.

(5) In the fcc to bcc transformation regime, the magnetization of the Fe films sharply increases. The magnetization of the transformed bcc Fe films is about four to five times larger than the extrapolated value from the low thickness fcc Fe films.

The paper is organized as follows. We describe the experimental details in Sec. II. Sections III and IV present the structural and the magnetic results, respectively. The correlation between the observed structural and magnetic proper-

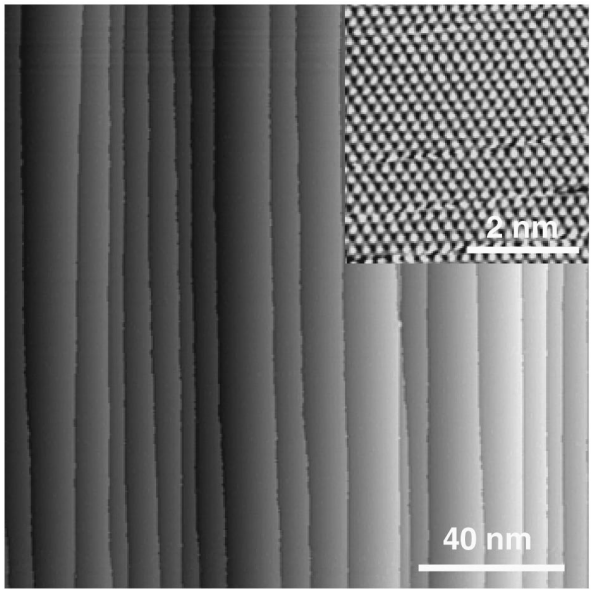

FIG. 1. STM topography image of a well-prepared Cu(111) vicinal surface. The atomic steps are parallel and oriented along ⟨011⟩ direction. The inset is an atomically resolved image (I_t = 0.25 nA, V_{bias} = 10 mV) recorded from a terrace showing the sixfold symmetry of the Cu(111) surface.

ties is discussed in Sec. V. The final conclusion will be drawn in Sec. VI.

II. EXPERIMENTAL DETAILS

The experiments were performed in a multichamber system including an MBE preparation chamber, an STM chamber, an analysis chamber equipped with facilities for Auger electron spectroscopy (AES), LEED and thin-film growth, and a MOKE chamber. The base pressure of the individual chambers is better than 5×10^{-11} mbar. The AES system has a cylindrical mirror analyzer (CMA) allowing the detecting limit to about 0.1 at. % for most of the elements. A fully automatic video-LEED system[16] has been used for recording LEED images as well as for measuring I/V LEED curves. In the present work the sample was prepared in the analysis chamber. The LEED and the AES measurements were taken immediately after film deposition. Then the sample was transferred to the MOKE chamber for magnetic measurements. STM images were recorded at room temperature after the MOKE study.

The copper substrate has a miscut of 1.2° with respect to the (111) orientation. The surface steps are aligned along one ⟨011⟩ direction with a (001) microfacet. The average terrace width is about 10 nm. Prior to film preparation the copper substrate was cleaned by Ar^+ sputtering and annealing cycles to 700 K. The crystallographic quality and the cleanliness of the substrate were monitored by LEED and AES, respectively. Both sharp LEED p(1×1) spots and the contamination-free Auger spectrum indicated the high quality of the substrate. The surface morphology of the substrate has also been examined by STM. As shown in Fig. 1, the surface consists of ⟨011⟩ oriented steps with an average ter-

The well-ordered atoms reflect the sixfold symmetry of the substrate surface, proving that the substrate surface is virtually defect free in the terraces.

The Fe films were prepared in the analysis chamber from an iron wire (5N in purity) heated by e-beam bombardment. At a typical Fe evaporation rate of 0.2 ML/min the pressure increased from 5×10^{-11} mbar to 1×10^{-10} mbar. To suppress interdiffusion, the copper substrate was kept at 0 °C during deposition.[17] Afterwards the sample was further cooled down to 170 K in order to avoid a temperature rise above 0 °C during transferring from the analysis chamber to the MOKE chamber.

In the MOKE chamber, the sample was placed on a manipulator with a function of three-axis movement as well as azimuthal rotation. The sample can be cooled down to 40 K and heated up to 600 K. In the present work most of the measurements were carried out in the sample temperature range between 90 and 270 K. Since the magnetization of nearly all the films persists above 270 K at which the interdiffusion starts to proceed, no attempts have been made to measure the Curie temperature in the present study. The polar and in-plane Kerr measurements are easily achieved by rotating the manipulator to allow the sample surface to be perpendicular or parallel to the external field. The maximum field is about 0.8 T, which appears to be large enough to saturate the films with thickness below 5 ML along the hard-axis direction.

III. MORPHOLOGY AND STRUCTURE

Figure 2 shows a series of STM topography images of Fe/Cu(111) films of different thickness. It is immediately visible that in the submonolayer regime (0.3 ML, 0.8 ML) the films have a quasi-1D form. The stripes are aligned parallel to one another on the upper edges of the steps. Most of the regions of the stripes have a monolayer height at 0.3 ML and increase to a double-layer height at 0.8 ML. At 0.3 ML the amount of Fe atoms is so small that the stripes are virtually formed by segments which are only weakly linked. At 0.8 ML, most of the segments have coalesced and the stripes become much more continuous. The edges of the stripes are rather rough. This is because the Fe atoms have a tendency towards growth along all three ⟨011⟩ directions even though they have a preferential alignment along the direction of the step edges. In other words, the Fe stripes are virtually formed by triangular-shaped islands which are linearly arrayed and connected. Such kind of construction of the stripes appears to have some strong influence on their magnetic properties, in particular the magnetization relaxation process which will be discussed in Sec. V.

With increasing thickness the stripes become wider and finally percolate between 1.4 and 1.8 ML, as seen in Figs. 2(c) and 2(d). This percolation leads to a direct connection between most of the stripes (>90%). In the present work we refer such a percolation as a 2D percolation while the connection between the segments within each stripe, i.e., between 0.3 and 0.8 ML, will be named 1D coalescence. Here the 2D percolation, in reality, leads to a 1D to 2D morpho-

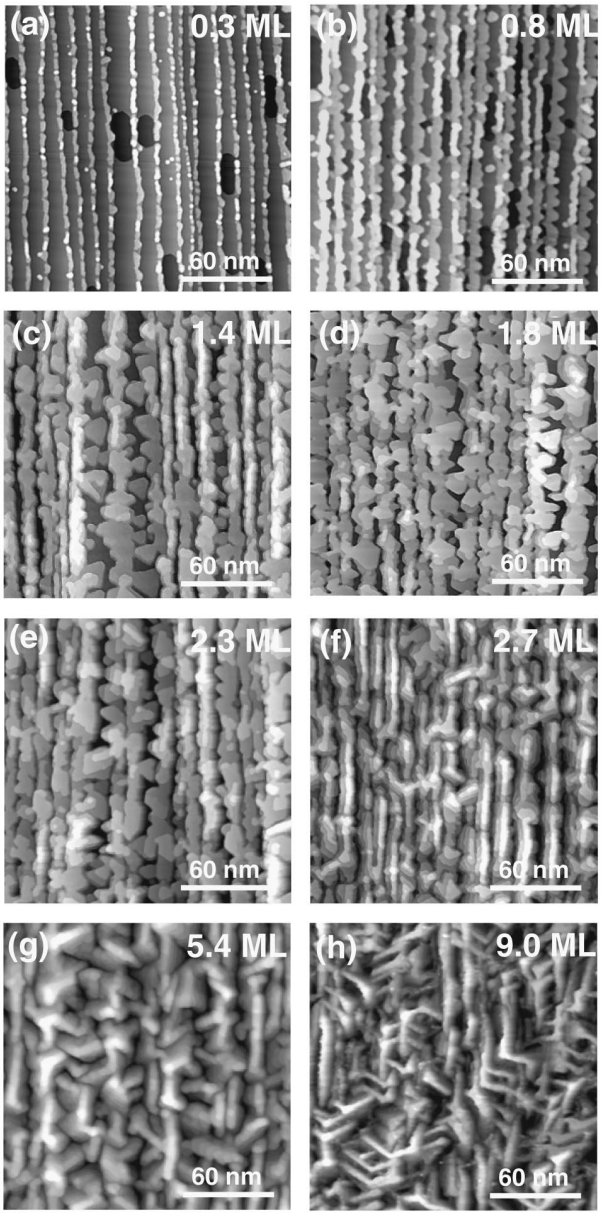

FIG. 2. Series of STM images showing the morphological evolution of the Fe/Cu(111) films with increasing thickness. In the submonolayer regime [(a) and (b)] the films have quasi-1D form. The 2D percolation occurs between 1.4 ML (c) and 1.8 ML (d). The morphology changes greatly between 2.3 ML (e) and 2.7 ML (f), as characterized by the formation of elongated domains aligning along the ⟨011⟩ directions.

Up to 2.3 ML the film morphology is characterized by triangular-shaped islands reflecting the threefold symmetry of the fcc (111) structure. As the islands are mostly bilayer or trilayer in height, the growth of the Fe/Cu(111) can be generally referred to as multilayer growth. Above 2.3 ML, the morphology of the films, however, changes significantly. The number of the exposed layers increases. It is 2 to 3 at 2.3 ML, 5 to 6 at 2.7 ML, and 7 to 8 at 9 ML. Moreover, the triangular-shaped islands are no longer visible in the images of the films with higher thickness [Figs. 2(e)–2(h)]. Instead

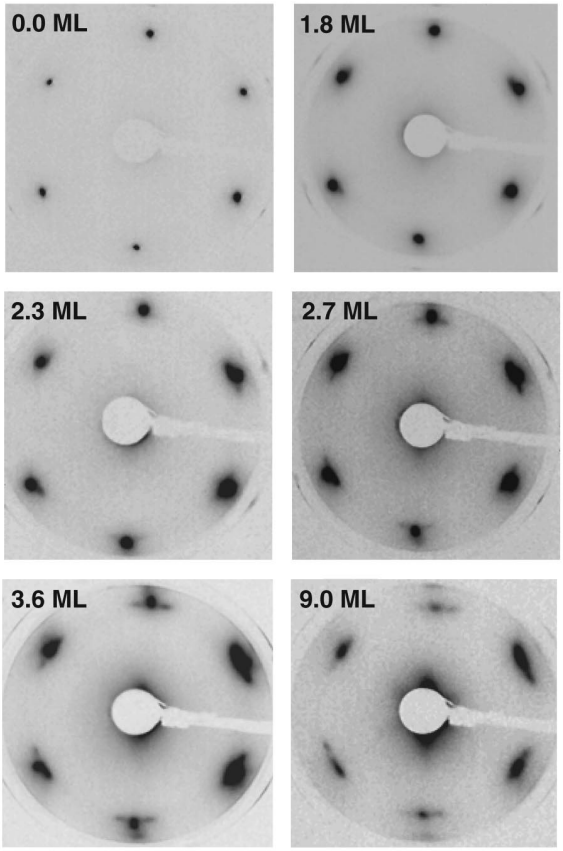

FIG. 3. LEED pattern of the Fe/Cu(111) films with different thickness. Below 2.3 ML the films have a p(1×1) pattern inherited from the substrate. From 2.3 ML on, satellite spots start to appear around the substrate spots. These satellite spots are caused by the bcc(110) domains with Kurdjumov-Sachs orientation.

ented along the step direction. But those along the other two ⟨011⟩ directions gradually develop to become almost equally important (see the 9.0 ML image in Fig. 2).

The question immediately arises: what causes the changes of the film morphology in the thickness regime between 2.3 and 2.7 ML? Since the triangular shape of the islands is a reflection of the fcc(111) symmetry, losing this feature might imply losing the fcc(111) structure. Indeed, our LEED studies have proven that the films undergo a fcc to bcc structural transition between 2.3 and 2.7 ML. Figure 3 shows the LEED patterns taken from different films at about 65 eV. The 1.4-ML and the 1.8-ML films have p(1×1) patterns with respect to the clean copper substrate, indicating the pseudomorphic growth of the Fe films. Because of the increased roughness owing to the multilayer growth, the films show more diffuse LEED spots than the copper substrate. With increasing thickness some additional spots start to appear around the substrate spots. At 2.3 ML these spots are already visible though their intensity is very weak. At 2.7 ML or even higher thickness the LEED patterns are already featured by these additional spots. In fact, these satellite spots are better seen at the beam energy of about 90 eV, as shown in the upper-left picture of Fig. 4 for the 2.7-ML film. There

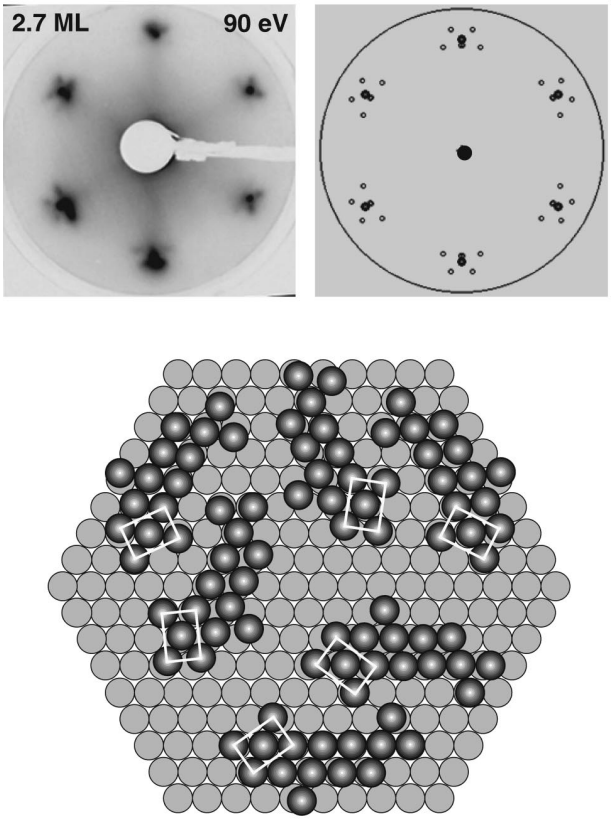

FIG. 4. Demonstration of the Kurdjumov-Sachs superstructure. Upper left: LEED pattern of the 2.7-ML film at the beam energy of 90 eV. Upper right: Simulated LEED pattern of Fe bcc(110) on Cu(111) with Kurdjumov-Sachs orientation. Note the consistency between the experimental and the simulated LEED patterns. Bottom: real-space schematic view of the six KS domains on the Cu(111) substrate.

has already been discussed in previous work that these spots result from the bcc(110) domains in Kurdjumov-Sachs (KS) orientation.[4] The KS orientation is a special case of the one-dimensional matching between bcc (110) and fcc(111) (bcc [111] is parallel to fcc [101]) with sides of the rhombic unit meshes of the film and the substrate to be parallel. Using the bulk parameters of Fe and Cu, we have simulated the LEED pattern of the KS orientation which is shown in the upper-right of Fig. 4. Except the middle two spots in the inner circle of the simulated pattern which are too close to be resolved experimentally, the experimental and the simulated LEED patterns agree well with each other. The six satellite spots reflect the six kinds of atomic relationship between the bcc(110) and fcc(111) structure as shown in the bottom picture of Fig. 4. Since these KS domains have only a one-dimensional matching with the substrate, each domain tends to have a narrow width in order to reduce the stress. In principle these six domains should have no preference on a flat surface due to the sixfold symmetry of the surface. Owing to the mirror symmetry, there are two kinds of domains along each ⟨011⟩ direction. As a result, the morphology of the films could be viewed as ridgelike structures oriented along the three ⟨011⟩ directions on a similar number. However, the

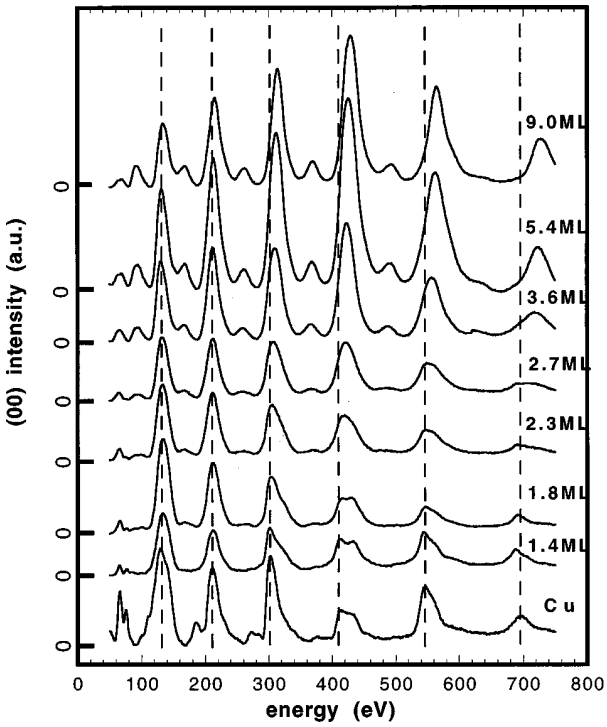

FIG. 5. IV-LEED spectrum of the (00) beam for the Fe/Cu(111) films. The 0's on the y axis indicate the zero level of the intensity of the corresponding curves after background subtraction. Below 2.3 ML there is no distinct peak shift. At higher thickness the peaks shift towards higher energies. The dashed lines indicate the peak position of the substrate.

tions [see the 2.7-ML image in Fig. 2(f)]. This can be explained by the fact that the substrate steps are oriented only in one of the ⟨011⟩ directions and therefore have introduced a twofold symmetry in addition to the sixfold symmetry of the fcc(111) surface. The two domain configurations which are parallel to the steps should be more favored as compared to the other four domains. The dominance of the two particular KS domains should, in principle, make the corresponding satellite spots have different intensity as compared to the rest satellite spots. However, as a result of the limited resolution and the rather rough surface, it is difficult to conclude this from our LEED data.

The structural transition from fcc to bcc is further analyzed by an IV-LEED study of the system. Figure 5 shows the (00) beam intensity vs energy curves for films with different thickness. These curves were obtained with the incident angle of the primary beam to be about 6° off the surface normal. In this case the step direction of the substrate is perpendicular to the plane of incidence. The dashed lines in Fig. 5 mark the peak position of the copper substrate. It is evident that with increasing thickness up to 2.3 ML there is no major shift of the peak position. There seems to be only one family of peaks inherited from the substrate (fcc), which is in stark contrast to the Fe/Cu(100) system where two families of peaks have been observed corresponding to fcc and fct, respectively.[8] Above 2.7 ML, the peaks have clearly shifted towards higher energies. Such a shift, within the kinematic approximation, indicates that the average interlayer

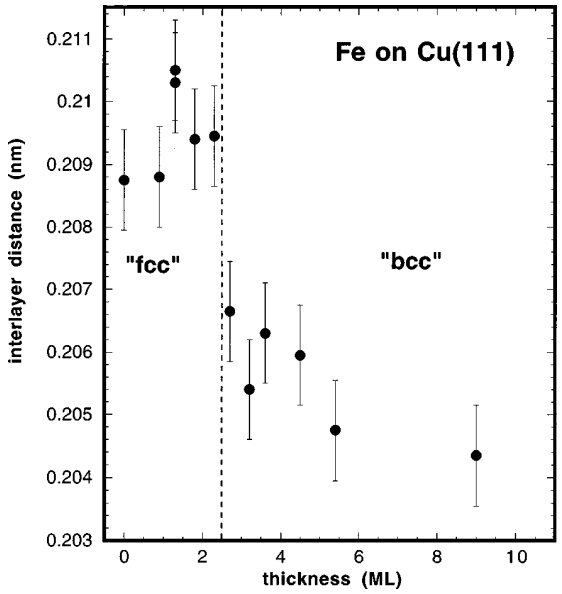

FIG. 6. The calculated interlayer distance from Fig. 5 using the kinematic approximation. It is evident that the interlayer distance decreases above 2.3 ML. The vertical dashed line separates films with different LEED structure. The films have a fcc-like structure below 2.5 ML, and a bcc structure above.

interlayer distance as a function of the film thickness. The results are shown in Fig. 6. Two regions can be clearly distinguished as indicated by the dashed line: in the low thickness region where the films show a p(1×1) pattern the interlayer distance of the films is close to that of the copper substrate, while in the high thickness region the interlayer distance of the films becomes apparently smaller. However, it has to be noted that the accuracy of the absolute value by our determination is influenced by the simple kinematic model, as the deviation of the calculated interlayer distance from the corresponding bulk value is about 0.001 and 0.003 nm for the fcc(111) and bcc(110), respectively. Nevertheless, the fact that the interlayer distance of the films drops down between 2.3 and 2.7 ML by more than 0.002 nm is quite unambiguous. This decrease of the interlayer distance is consistent with the LEED patterns which indicate the fcc to bcc structural transition between 2.3 and 2.7 ML.

The observed critical thickness of the fcc→bcc transformation is smaller than the previously reported value[4] of about 4 or 5 ML. This might be due to the fact that a vicinal copper substrate is used in the present work. Compared to the growth of Fe on a flat substrate, at the same nominal thickness the step decoration effect of the Fe growth on the vicinal substrate could make the films be locally thicker along the step edges. The fcc→bcc transformation could proceed first in these locally thicker regions. In addition, on the vicinal surface the islands have an elongated shape along one of the ⟨011⟩ directions (the step direction) even before the structural phase transformation. These elongated islands may have an easier path to convert into bcc KS domains as compared to the normal triangular-shaped islands on a flat Cu(111) surface. This is in fact backed by our STM observations that the bcc domains along the step direction appears

mation (about 2.7 ML) most of the bcc domains are oriented along the step direction. The number of the bcc domains oriented along the other two ⟨011⟩ directions only become significant at higher thickness (e.g., see the 5.7-ML image in Fig. 2). Therefore, it is not surprising that the Fe films on the vicinal Cu(111) substrate transform into bcc structure at lower thickness than the films on a flat Cu(111) substrate.[18]

IV. MAGNETIC PROPERTIES

As shown in Fig. 2, in the submonolayer regime the Fe/Cu(111) films have a quasi-1D form. In our previous polar MOKE measurements we have shown that these Fe stripes exhibit hysteresis with a coercivity depending strongly on the temperature.[2] The easy magnetization axis of the stripes is determined to be perpendicular to the surface, because no magnetic signal was detected in the longitudinal geometry, irrespective of the external field being parallel or perpendicular to the stripes. In the same work we have also performed time-dependent magnetization measurements by MOKE. The results obtained from the stripes, which has a submonolayer nominal coverage (~0.8 ML), showed that at zero field the magnetization decays at a speed strongly depending on the temperature. For example, while the magnetization of the 0.8-ML stripes decays very slowly at about 100 K, it decays rapidly to zero (within 20 sec) at 160 K. We associated the decay of the magnetization with the superparamagnetic nature of the 1D stripes. The fact that the superparamagnetic stripes exhibit hysteresis is simply because the measuring time of the magnetization curves is considerably shorter than the magnetization relaxation time of the stripes.

Here we extend the previous work by demonstrating the coverage-dependent magnetization relaxation process of the Fe/Cu(111) films. Figure 7 shows the magnetization relaxation curves of films with different thickness ranging from that of the 1D stripes to the 2D percolated film. All the curves were measured in the polar geometry. The 0 level of each curve indicates the signal of a demagnetized state of the films. An external field of about 0.6 T was applied at the time point which is marked as ''field on.'' For all the films the magnetization quickly reaches saturation. The external field was removed at the time point marked as ''field off.'' In all three cases the magnetization falls down, but with distinctly different speed. At 160 K, the magnetization of the 0.8-ML film decays down to zero within 20 sec. In contrast, at the same temperature after an initial quick decay the residual magnetization of the 2-ML film is much more stable. The quickest decay of the magnetization is observed, however, for the 0.3-ML film. Its magnetization decays rapidly to zero in a few seconds even at much lower temperature of 50 K. The different behavior of the magnetization relaxation process of these films appears to be closely correlated with their morphology, which will be discussed in the next section.

We now turn to consider the magnetic anisotropy of the Fe/Cu(111) films. As mentioned above, the easy magnetization axis of the submonolayer films (the stripes) is perpendicular to the film surface. This in fact has been found to be the case for all the films below 2.3 ML of thickness. Figure

DOCKET ALARM

Explore Litigation Insights

Docket Alarm provides insights to develop a more informed litigation strategy and the peace of mind of knowing you're on top of things.

Real-Time Litigation Alerts

Keep your litigation team up-to-date with **real-time alerts** and advanced team management tools built for the enterprise, all while greatly reducing PACER spend.

Our comprehensive service means we can handle Federal, State, and Administrative courts across the country.

Advanced Docket Research

With over 230 million records, Docket Alarm's cloud-native docket research platform finds what other services can't. Coverage includes Federal, State, plus PTAB, TTAB, ITC and NLRB decisions, all in one place.

Identify arguments that have been successful in the past with full text, pinpoint searching. Link to case law cited within any court document via Fastcase.

Analytics At Your Fingertips

Learn what happened the last time a particular judge, opposing counsel or company faced cases similar to yours.

Advanced out-of-the-box PTAB and TTAB analytics are always at your fingertips.

API

Docket Alarm offers a powerful API (application programming interface) to developers that want to integrate case filings into their apps.

LAW FIRMS
Build custom dashboards for your attorneys and clients with live data direct from the court.

Automate many repetitive legal tasks like conflict checks, document management, and marketing.

FINANCIAL INSTITUTIONS
Litigation and bankruptcy checks for companies and debtors.

E-DISCOVERY AND LEGAL VENDORS
Sync your system to PACER to automate legal marketing.